

Shear-Induced Alignment of Smectic Side Group Liquid Crystalline Polymers

Stanley Rendon and Wesley R. Burghardt*

Department of Chemical and Biological Engineering, Northwestern University, Evanston, Illinois 60208

Maria L. Auad and Julia A. Kornfield

Department of Chemistry and Chemical Engineering, California Institute of Technology, Pasadena, California 91125

Received December 19, 2006; Revised Manuscript Received July 7, 2007

ABSTRACT: Large amplitude oscillatory shear (LAOS) is frequently capable of generating macroscopic alignment from an initially random orientation distribution in ordered polymer fluids. Side-group liquid crystalline polymers are of special interest in that the flow field may couple differently to the polymer backbone and the mesogen ordering. We report combined rheological and in situ X-ray scattering investigations of LAOS-induced alignment in smectic side-group LCPs. Synchrotron X-ray scattering is used to study orientation development using a rotating disk shear cell in which orientation is tracked within the flow-vorticity (1–3) plane. In all cases, we find that shear promotes anisotropic orientation states in which the lamellar normal tends to align along the vorticity direction of the shear flow (“perpendicular” alignment). We examine the effects of shear strain amplitude and polymer backbone molecular weight on the ability of LAOS to induce alignment. Rheological measurements of the dynamic moduli reveal that large amplitude shearing in the smectic phase causes a notable decrease in the modulus. X-ray and rheological data demonstrate that increasing strain promotes higher degrees of orientation, while increasing molecular weight impedes development of smectic alignment.

1. Introduction

The inherent anisotropy and long range orientational order of liquid crystalline polymers (LCPs) renders them useful in a range of applications that require a high degree of macroscopic orientation. Thermotropic LCPs may be broadly divided into two classes depending on how rigid mesogenic moieties are incorporated into the polymer molecules. In main-chain LCPs (MCLCPs), mesogenic groups are directly incorporated as part of the polymer backbone, while in side-group LCPs (SGLCPs) mesogenic units are decoupled from the polymer backbone, typically by flexible hydrocarbon spacers.

Commercial applications of MCLCPs exploit their high mechanical strength, thermal stability, high chemical resistance, low melt viscosity, and low density change upon solidification.¹ To some degree, these favorable attributes all result from the spontaneous ordering of rigid molecules into liquid crystalline phases. Mechanical properties of MCLCP products are further strongly influenced by the macroscopic molecular orientation state induced by flow fields during processing.² While MCLCPs exhibit much more complex rheology than conventional flexible polymers,³ the direct incorporation of mesogens into the polymer backbone means the orientational dynamics of the polymer backbone and mesogenic units are intimately coupled.⁴ At the same time, use of LCPs in technologies which exploit the anisotropic optical properties of liquid crystalline phases often require external manipulation of mesogen orientation. Main-chain materials are poorly suited to such applications, since mesogen reorientation requires large scale changes in the polymer backbone conformation. SGLCPs are more naturally suited to such applications provided the attaching spacers are sufficiently long to partially decouple the dynamics of the rigid

mesogenic side groups from the that of the polymer backbone. However, this increases the possible complexity in the flow behavior of these polymers, since incompatibility can now arise between a flow's separate effect on polymer backbone conformation and mesogen orientation (as characterized by the liquid crystal director, \mathbf{n}).^{5–7}

SGLCPs are considered to have significant potential in the areas of nonlinear optics and data storage.⁸ Such applications typically require macroscopic orientation of the liquid crystalline phase.⁹ In low molecular weight LCs, generating and manipulating orientation can be usually achieved through combinations of surface treatments and applied electric or magnetic fields. However, these methods become impractical when trying to orient high molecular weight SGLCPs. It is well-known that shear flow can be highly effective in inducing macroscopic alignment in materials such as MCLCPs and block copolymers.^{4,10} However, early reports by Zentel and Wu¹¹ suggested that shear flow was incapable of inducing orientation in *nematic* SGLCPs since the rheology was dominated by the flexible polymer backbone.^{12,13} Contrary to these results, Kannan et al.^{14,15} and Rubin et al.¹⁶ demonstrated that large amplitude oscillatory shear (LAOS) could be used as a means of inducing net macroscopic alignment of *nematic* SGLCPs. This conclusion was based on the observation that at the isotropic–nematic transition there was a noticeable decrease in the dynamic moduli and that shearing in the nematic phase resulted in high levels of transparency and birefringence. However, quantitative measurements of the degree of alignment were not obtained.

While shear flow behavior of *nematic* SGLCPs has been an area of active research, comparatively few studies have been made on the shear-induced alignment of *smectic* SGLCPs. Rubin and co-workers¹⁶ demonstrated that application of LAOS resulted in an overall decrease in the dynamic modulus, G^* , a frequent indicator of flow-induced orientation in ordered fluids;

* Author to whom correspondence should be addressed. E-mail: w-burghardt@northwestern.edu.

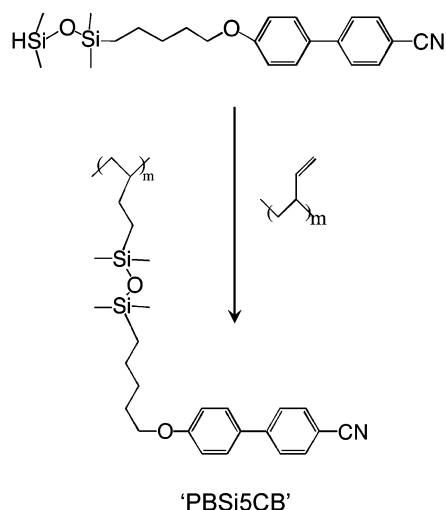


Figure 1. Schematic illustration of PBSiCB5 synthesis, showing mesogen attachment to 1,2-polybutadiene backbone. Full details of synthetic procedure may be found in ref 24.

Werwerka et al. report similar observations for other nematic and smectic SGLCPs.¹⁷ Indeed, there is ample evidence that layered fluids as a class are highly susceptible to the orienting influence of LAOS. Larson et al.¹⁰ studied the rheology of lamellar block copolymers and smectic thermotropic and lyotropic liquid crystals under the influence of LAOS and determined that, in the smectic state, large strain amplitudes are capable of inducing higher degrees of alignment evidenced by remarkable reductions in dynamic moduli. However, it is also found that layered fluids may evolve toward different orientation states depending on the particular characteristic of the material and the flow conditions.^{18,19} While rheological changes induced by LAOS can be useful indicators of flow-induced orientation, direct structural characterization of the alignment process is obviously preferable. It is also important to recognize that dynamic modulus data collected on textured samples cannot readily be interpreted in terms of underlying fundamental elastic and viscous constants characterizing the smectic phase. In the literature and in the present work, however, such data are highly useful as a sensitive indicator of changes in the orientation state.

There have been limited studies that directly assess flow-induced structure in smectic side-chain liquid crystalline polymers during shear flow. Noirez and Lapp used in situ neutron scattering to study chain conformations during steady shear near a nematic–smectic transition.²⁰ Wiberg and co-workers used infrared dichroism to monitor mesogen alignment in a SGLCP during steady shear, also in unidirectional shear.²¹ Hamley and co-workers have monitored SGLCP smectic layer orientation in LAOS using X-ray scattering.^{22,23} Here we report recent investigations of the shear-induced alignment of smectic side-group liquid crystalline polymers under the influence of LAOS using combined rheological and in situ X-ray scattering techniques. This research builds on previous work in which cyanobiphenyl-based side-group LCPs that display smectic mesophases were synthesized and characterized.²⁴ The wide range of available polymers allows the role of polymer backbone molecular weight on shear alignment processes to be investigated.

2. Experimental Section

2.1. Materials. The side-group LCPs studied in this investigation are in a series designated “PBSiCB5” (Figure 1). The synthesis begins with a monodisperse 1,2-polybutadiene main-chain polymer

backbone which is then linked to cyano-biphenyl mesogenic side groups via short, flexible siloxane spacers. These side-group LCPs exhibit a smectic mesophase at temperatures below 60 °C. The SGLCP samples examined included polymer molecular weights of 518 kg/mol with polydispersity of $M_w/M_n = 1.59$ (sample 518K PBSiCB5), 690 kg/mol with $M_w/M_n = 1.83$ (sample 690K PBSiCB5), and 1900 kg/mol with $M_w/M_n = 1.90$ (sample 1900K PBSiCB5). Greater polydispersity emerges in higher molecular weight samples due to an increased likelihood of occasional chain coupling during the side-chain attachment reaction. The smectic–isotropic transition temperature of these polymers is somewhat affected by the combined effects of molecular weight distribution and incomplete attachment of mesogens; for the samples studied here, the transition occurs across a biphasic region with a clearing temperatures near 65 °C. Further details on the synthesis and phase behavior of these SGLCP samples are described in a previous publication.²⁴

2.2. Rheology. Rheological testing was performed in a Rheometrics Solids analyzer (RSA II and RSA III) dynamic mechanical testing systems which have been customized for rheo-optical studies.²⁵ Here, however, only mechanical data are reported. A “shear-sandwich” geometry was used to perform rheological measurements, using custom fixtures with the plates replaced by CaF₂ windows. The tool area used was 2 cm². The gap thickness varied from sample to sample and ranged from 0.32 to 0.55 mm. Environmental control was achieved by circulating air or nitrogen through the environmental chamber. The uniformity and stability of the temperature were specified to be ± 0.5 °C.

In order to erase any prior thermal/mechanical history and provide a reproducible initial condition, samples were heated well into the isotropic phase (80–85 °C) and held there for 10 min prior to each shearing experiment. Samples were then cooled into the smectic phase (60 °C) resulting in a random “polydomain” texture. Rheological testing involved three types of oscillatory shear experiments: (1) strain sweeps, used to define the linear response range of the materials (<5% strain), (2) frequency sweeps, to investigate the equilibrium dynamics of the material with strains within the linear range, and (3) prolonged shearing, to probe smectic layer alignment using large amplitude oscillatory shear (LAOS) at a fixed frequency and strain for an extended time period. A standard protocol of 90 oscillation cycles was used for all experiments. Initial experiments were performed at a frequency of 0.1 rad/s; additional experiments were later performed at 0.314 rad/s to match the conditions of the in situ X-ray scattering experiments (see below). Frequency sweeps were coordinated with prolonged large amplitude shearing experiments in the smectic phase such that the dynamics of the side-group samples could be probed before and after the influence of LAOS.

2.3. X-ray Scattering. Small-angle X-ray scattering was used to complement the rheological results by probing flow-induced changes in smectic-layer orientation in the “1–3” (flow–vorticity) plane of the shear flow. LAOS was applied to the SGLCP samples using a Linkam CSS-450 high-temperature shearing stage, which employs a rotating disk-shearing geometry. A description of the modifications to render the shearing stage suitable for X-ray studies is provided elsewhere.²⁶ All synchrotron X-ray scattering measurements were carried out at beamline 5BM-D of DND-CAT at the Advanced Photon Source (APS) of Argonne National Laboratory, using a photon energy of 20 keV. A CCD detector (MarCCD) was used to collect 2-D digitized X-ray scattering patterns.

2.4. X-ray Data Collection and Analysis. Prior to each LAOS experiment, samples were thermally cleared by heating to 85 °C and holding for 10 min. The temperature was then cooled to 60 °C, within the smectic phase.²⁴ Samples were subjected to large-amplitude oscillatory shear at a fixed frequency of 0.05 Hz ($\omega = 0.314$ rad/s; we found that the Linkam shear stage could not reliably apply oscillatory shear at the lower frequency of 0.1 rad/s), and shear strain amplitudes ranging from 50% to 200%. X-ray scattering patterns were collected continuously during the shearing to study the evolution of orientation state. Exposure times of 20 s were used, so that each pattern reflects an average of the fluid structure over

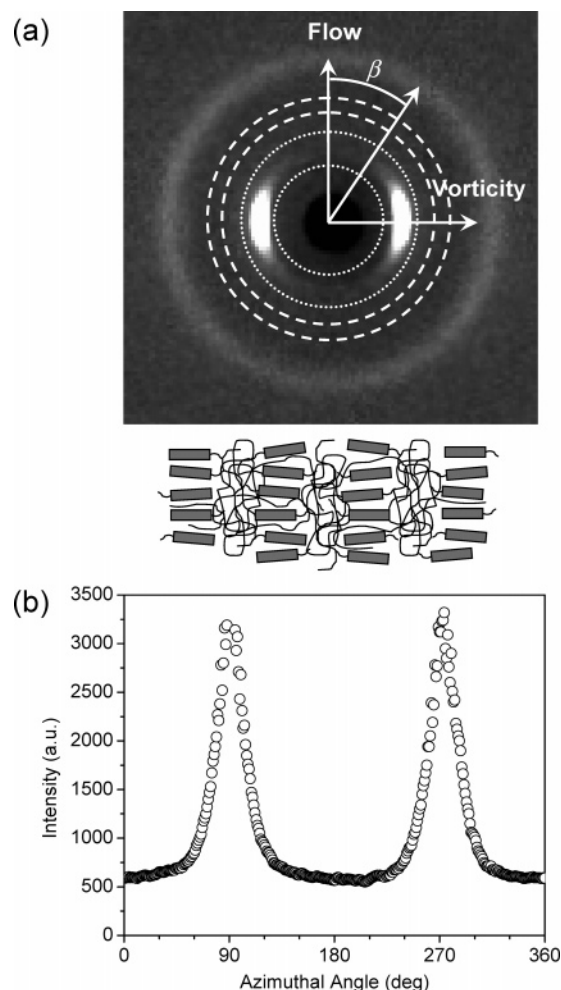


Figure 2. (a) Representative X-ray scattering pattern and (b) azimuthal intensity scan for 518 kg/mol PB5iCB5 during oscillatory shear. Depicted on the X-ray image are the q ranges used to extract the azimuthal scan of smectic peak intensity (•••), and, at somewhat higher q , to compute a baseline correction intensity value (---). The cartoon illustrates the perpendicular alignment of smectic layers indicated by the pattern in part a.

one full cycle of oscillatory shear. In some cases, data acquisition continued after cessation of LAOS to study subsequent relaxation of the flow-induced alignment.

In the small-angle regime, X-ray patterns show sharp smectic layer reflections that are rendered anisotropic by shear (Figure 2). In all cases, application of LAOS caused the smectic reflection to become concentrated along the vorticity direction, indicative of a perpendicular character to the macroscopic orientation state. (Hamley et al. report perpendicular alignment during LAOS, but in their study significant alignment was only achieved at much higher frequencies than those studied here.²²) At somewhat larger angles, an isotropic scattering ring is observed, which is attributed to diffraction from the Kapton windows employed in the shear cell. At still larger angles, diffuse peaks indicative of lateral mesogen packing are also apparent;²⁴ here, we concentrate on the small-angle regime to concentrate specifically on the alignment the smectic layers. To account for possible drifts in the incident flux over the course of an experiment, each image was normalized using the integrated Kapton peak intensity as a surrogate for the incident beam intensity. The degree of smectic layer alignment was characterized using azimuthal scans of intensity $I(\beta)$ averaged over a finite range of the scattering wave vector, q , around the smectic layer reflection (Figure 1). Prior to extraction of azimuthal scans, a baseline was subtracted to correct for background scattering (e.g., air, X-ray windows, etc.). The baseline value was based on an

average intensity measured in a featureless region of the scattering pattern at slightly higher q than the smectic reflection (Figure 1).

Methods for analyzing azimuthal data of this sort often rely on an assumption of uniaxial distribution of orientation about a predefined symmetry axis, conditions that are not generally met during induced shear flow experiments.^{27,28} (Critical assessment of the three-dimensional character of the orientation state would require study in multiple shear flow planes; unfortunately, limited sample quantities have prevented use of a separate shear cell to provide complementary data in the flow-gradient (1–2) plane.³⁶) To quantify the degree of smectic layer alignment in the “1–3” plane, we have instead adopted a simpler method of characterizing anisotropic X-ray scattering patterns in terms of a second moment tensor analysis of the azimuthal scan.²⁹ Each point on the azimuthal scan is represented by a unit vector, \mathbf{u} , such that $u_1 = \cos \beta$ and $u_2 = \sin \beta$ (where β is the azimuthal angle), and anisotropy is characterized in terms of the second moment of \mathbf{u} weighted by the observed intensity distribution:

$$\langle \mathbf{u}\mathbf{u} \rangle = \begin{bmatrix} \langle u_1 u_1 \rangle & \langle u_1 u_2 \rangle \\ \langle u_1 u_2 \rangle & \langle u_2 u_2 \rangle \end{bmatrix} = \begin{bmatrix} \langle \cos^2 \beta \rangle & \langle \sin \beta \cos \beta \rangle \\ \langle \sin \beta \cos \beta \rangle & \langle \sin^2 \beta \rangle \end{bmatrix} \quad (1)$$

The brackets $\langle \dots \rangle$ denote an average weighted by the azimuthal intensity scan $I(\beta)$. For example, the 11-component of $\langle \mathbf{u}\mathbf{u} \rangle$ is given by

$$\langle \cos^2 \beta \rangle = \frac{\int_0^{2\pi} \cos^2 \beta I(\beta) d\beta}{\int_0^{2\pi} I(\beta) d\beta} \quad (2)$$

Anisotropy in the orientation state is then characterized via flow induced changes in the components of $\langle \mathbf{u}\mathbf{u} \rangle$. We define an “anisotropy factor” as the difference in the principal values of $\langle \mathbf{u}\mathbf{u} \rangle$. For measurements in the flow-vorticity plane of shear flow, symmetry dictates that the off-diagonal components of $\langle \mathbf{u}\mathbf{u} \rangle$ must be zero, so anisotropy factor may be simply defined as

$$AF = \langle u_2 u_2 \rangle - \langle u_1 u_1 \rangle = \langle \sin^2 \beta \rangle - \langle \cos^2 \beta \rangle \quad (3)$$

The ordering in this definition anticipates the perpendicular character of the alignment, such that perfect perpendicular alignment (sharp peaks at $\beta = 90^\circ$) would yield an anisotropy factor of +1. The random “polydomain” initial condition is associated with $AF = 0$. Thus defined, the anisotropy factor bears similarity to molecular order parameters, which range between 0 and 1, representing the local degree of mesogen ordering in nematic and smectic liquid crystals. We emphasize that the present analysis specifically addresses only the degree of *smectic layer* alignment within the 1–3 plane.

We do not observe any changes in smectic peak position (e.g., d -spacing) associated with shear-induced alignment. While shear-induced layer spacing changes have been documented in lower molecular weight smectic SGLCPs that exhibit parallel alignment,³⁴ this finding agrees with previous observations of negligible layer spacing changes in samples which show perpendicular alignment.^{23,34}

3. Results and Discussion

3.1. Rheological Studies. 3.1.1. Effect of Strain. Large amplitude oscillatory shear leads to a progressive reduction in the apparent storage modulus measured during shear (Figure 3). The data exhibit a rapid initial decay over approximately the first 500 s, followed by a more gradual decrease during the remainder of the experiment. The decrease in the storage modulus of 518K PB5iCB5 over time is consistent with general observations in layer like fluids such as smectic liquid crystals and lamellar block copolymers. Shear orientation dynamic studies in small-molecule smectics (4-cyano-4'-octylbiphenyl) have shown that large amplitude oscillations will cause a

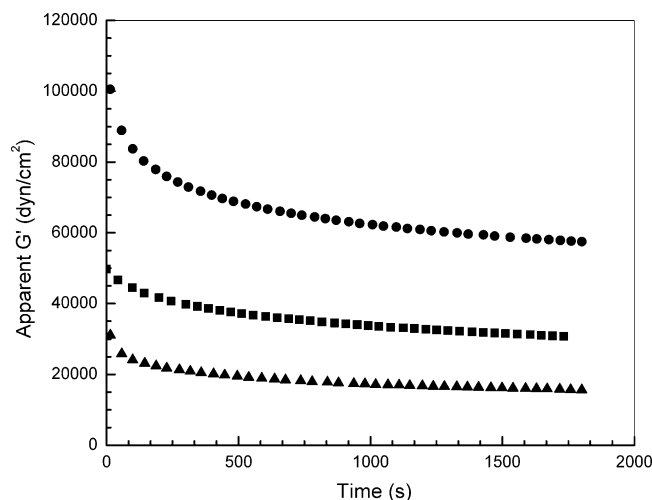


Figure 3. Apparent storage modulus as a function of time for 518 kg/mol PBsICB5 during LAOS at 0.1 rad/s and 50% strain (●), 95% strain (■), and 200% strain (▲).

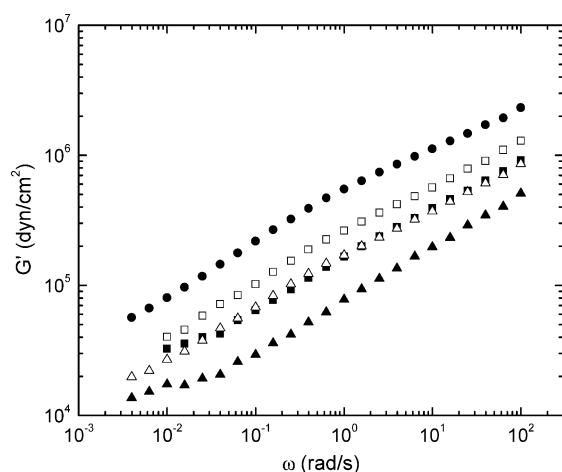


Figure 4. Storage modulus as a function of frequency for 518 kg/mol PBsICB5 under conditions of no preshear (●), after 90 cycles of LAOS at 0.314 rad/s, 95% (■) and 200% strain (▲), and after 3 h of relaxation following LAOS at 0.314 rad/s, 95% (□) and 200% strain (△).

decrease in the magnitude of the nonlinear complex modulus at strain amplitudes of order unity.¹⁰ More specifically, these results mirror progressive reductions in apparent storage modulus observed during LAOS of both nematic¹⁵ and smectic¹⁷ SGLCPs.

Because the data in Figure 3 were collected in the nonlinear regime, it is difficult to interpret the response in terms of the underlying smectic layer structure. A better way of probing flow induced structure is to measure the *linear* response of the material after having induced LAOS and compare it to the original response prior to shear alignment. As anticipated by Figure 3, 90 oscillation cycles at large strain do lead to a substantial reduction of the linear storage modulus, G' (Figure 4). The drop in G' observed after carrying out LAOS at 200% strain was larger than that for 95% strain, suggesting a higher degree of alignment. Similar reductions in linear storage modulus following application of LAOS have been reported in smectic SGLCPs by both Rubin et al.¹⁶ and Werwerka et al.¹⁷ Modulus reduction in layered fluids subject to LAOS is frequently attributed to the natural promotion of alignment in a direction that minimizes the viscosity of layered fluids, and perhaps also to a reduction in the density of defects.³ In contrast to these results, Hamley and co-workers observed in their system that the linear viscoelastic properties rebounded quickly to their

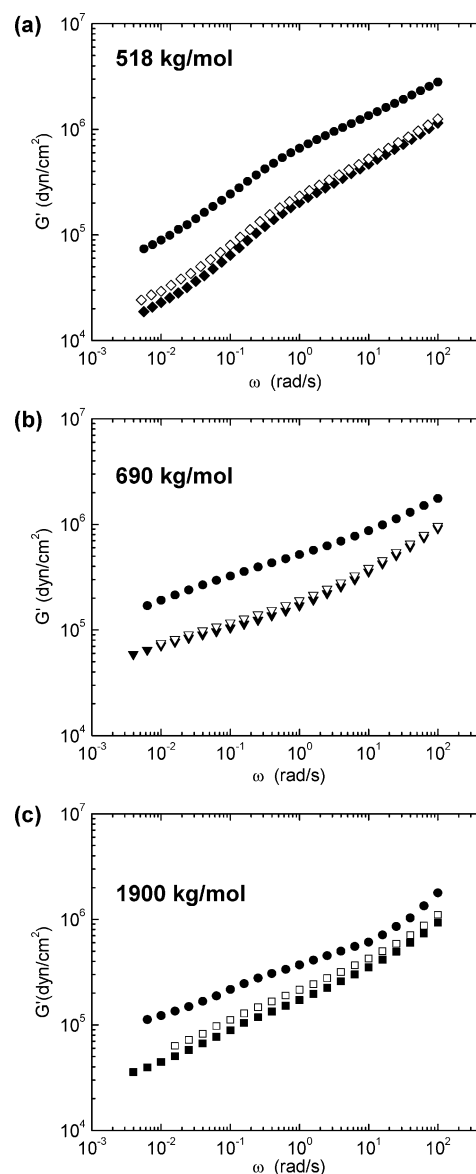


Figure 5. Effect of molecular weight on the frequency dependent storage modulus for: (a) 518, (b) 690 and (c) 1900 kg/mol PBsICB5 samples. For each SGLCP sample, data were collected under conditions of: no-preshear (●); after 90 cycles of LAOS at 0.1 rad/s, 95% strain (closed symbols); and after 3 h of relaxation following LAOS at 0.1 rad/s, 95% strain.

pre-LAOS values upon reduction in strain, despite direct evidence of flow-induced alignment of smectic layers.²²

Linear dynamic moduli data were also obtained on the same shear-aligned samples after 3 h of relaxation (Figure 4). The relaxed data (open symbols) show some recovery of storage modulus on this time frame. Similar recovery of moduli toward unaligned values following cessation of LAOS have been reported in both nematic¹⁵ and smectic¹⁷ SGLCPs. These results suggest the possibility that the quality of layer alignment degrades with time during the relaxation period, although this interpretation was not tested via direct measurements of the degree of alignment in either system.

3.1.2. Effect of Molecular Weight. Frequency sweep experiments were carried out on SGLCP samples of varying molecular weight, both prior to and following LAOS at 95% strain (Figure 5). The evolution of the storage modulus over the entire frequency domain studied follows in close agreement with data previously shown in Figure 4. Following application of LAOS G' again drops relative to data measured in a quiescent

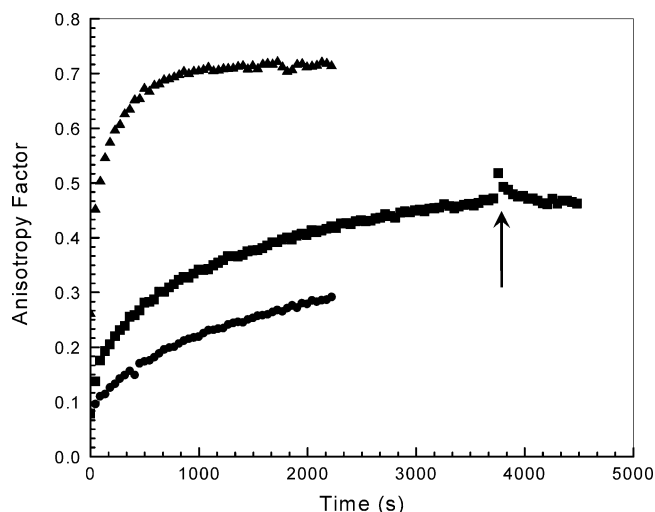


Figure 6. Anisotropy factor as a function of time following inception of LAOS for 518 kg/mol PBSCB5 at 0.314 rad/s and 50% strain (●), 95% strain (■), and 200% strain (▲). The arrow indicates point of cessation of LAOS in the 95% strain experiment.

polydomain sample. The similarity in response across this entire range of molecular weight suggests that these changes induced in the linear rheology result from a common mechanism associated with the smectic layers, with no significant effect of sample molecular weight.

In contrast to the results presented above, only small amounts of recovery in G' are observed here after 3 h of relaxation (Figure 5; open symbols). The lower frequency employed in Figure 5 (0.1 rad/s) means that the total time elapsed during shearing is over three times longer in the present case. It is possible that the longer exposure to LAOS results in a less defective alignment state in which subsequent relaxation occurs more slowly.

3.2. X-ray Scattering Studies. 3.2.1. Effect of Strain. The degree of smectic layer alignment of the PBSCB5 side-group LCP samples was probed along the 1–3 flow-vorticity plane under the influence of LAOS. Strain was found to have a strong effect on the degree of smectic layer alignment in the 518K PBSCB5 sample (Figure 6). At the two lower strains (50 and 95%) anisotropy increases monotonically for the duration of the shearing. At 200% strain, however, anisotropy eventually saturates at a steady value of $AF \approx 0.7$. The increase in flow-induced alignment of smectic layers with shear strain is consistent with rheological data presented in Figure 4 that show larger decreases in linear modulus when this sample is subjected to LAOS with larger strain amplitudes. In addition to higher degree of alignment, Figure 6 demonstrates that the kinetics of flow alignment is substantially accelerated at higher strains, reaching a final value within about 1000 s, while for the smaller strains, the orientation continues to evolve for the duration of the experiment.

As demonstrated in Figure 2, LAOS promotes an orientation state in which diffraction from the smectic layers becomes concentrated along the vorticity direction of the shear flow, corresponding to alignment of smectic layers in the “perpendicular” direction, with layer normals parallel to the vorticity axis of the shear flow. Figure 6 demonstrates that a high degree of orientation may be achieved at large strain. Our observation of perpendicular alignment in this smectic SGLCP is consistent with previous observations reported by Wiberg et al.²¹ and Hamley et al.²² indicating perpendicular alignment in steady or large-amplitude oscillatory shear flow, respectively. In layered fluids, the two orientation states most likely to emerge during

shear are “parallel” (with the layer normal parallel to the gradient direction) and “perpendicular” (with the layer normal parallel to the vorticity axis);³ in either of these orientations, shear deformation does not intrinsically promote any change in spacing of a layered fluid. On the other hand, molecular connectivity *between* layers may be expected to strongly promote the perpendicular orientation over parallel, since only perpendicular alignment eliminates the need for substantial molecular scale rearrangements to realize shear deformation. In the case of block copolymers, this is vividly illustrated by work by Vigild et al.,³⁰ who found a strong bias toward perpendicular orientation in pentablock copolymers. Similarly, smectic ordering in main-chain liquid crystalline polymers (necessarily with highly connected layers) has been found to promote perpendicular orientation of the layers.^{31,32} (Interestingly, in each of these cases, sufficiently strong flow is able to induce a transition to an otherwise unexpected “transverse” orientation state due to alignment of the backbone molecular orientation along the flow direction.^{30,32}) Chain conformations in smectic SGLCPs are oblate relative to the layer normal, due to the tendency of chains to orient perpendicular to the mesogens.³³ However, for sufficiently high molecular weight, the polymer backbone should pass through multiple layers, providing the connectivity necessary to promote perpendicular alignment by this mechanism. In this respect it is interesting that Noirez observed parallel layer alignment under shear in a lower molecular weight smectic SGLCP, but that perpendicular alignment was found in a higher molecular weight sample.³⁴ While primarily finding perpendicular orientation, Castelletto et al. also observed the unexpected transverse alignment in a smectic SGLCP during LAOS following a particular thermal history;²³ here, we have found only the more conventional perpendicular alignment.

Anisotropy was also monitored upon cessation of flow for the case of sample 518K PBSCB5 in order to determine the extent of the smectic layer relaxation (Figure 6). After shearing at 95% strain for over an hour and then stopping the flow, a slight jump in anisotropy factor was observed. However, the anisotropy quickly returned close to its value prior to flow cessation. Because of limits in the available synchrotron beam time, we were unable to follow relaxation for extended time periods to assess the extent to which evolution in linear dynamic moduli over long relaxation periods (e.g., Figure 4) were associated with changes in the orientation distribution of the smectic layers.

3.2.2 Effect of Molecular Weight. Transient measurements of anisotropy were carried out for several SGLCP samples with differing molecular weight (Figure 7). As was already seen, the lowest molecular weight sample, 518K PBSCB5, readily aligns in LAOS at a strain of 95%, with steadily increasing anisotropy factor. In the highest molecular weight sample (1900K PBSCB5), however, orientation development is suppressed at this strain (Figure 7a). After a rapid initial increase, the anisotropy factor fails to grow much above 0.1. Experiments on the intermediate molecular sample (690K PBSCB5), not surprisingly, fall between those of the other two samples. However, while good reproducibility was found in the 518 and 1900K samples, repeated experiments in the 690K material led to data with systematic differences (Figure 7a). We have no explanation for this, except to note that in all cases there was a small initial bias in the orientation state resulting from cooling the sample in the shear cell from the isotropic phase. It is possible that some difference in the initial orientation state between these repeated experiments persisted throughout their duration. Similar

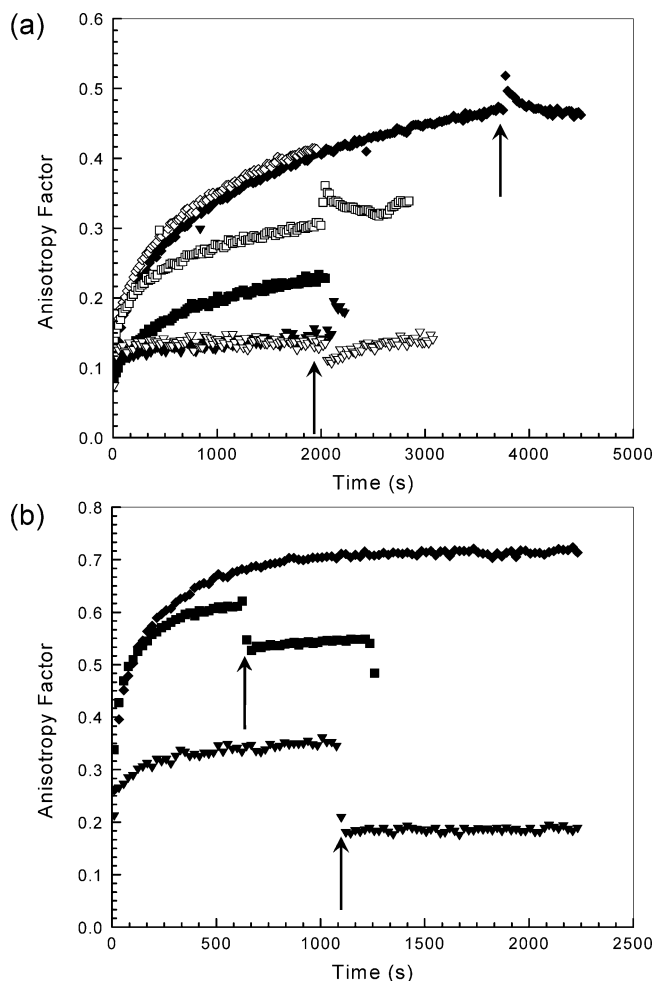


Figure 7. Anisotropy factor as a function of time during LAOS at 0.314 rad/s and strains of (a) 95%, and (b) 200%, for 518 kg/mol PBSiCB5 (\blacklozenge , \diamond), 690 kg/mol PBSiCB5 (\blacksquare , \square), and 1900 kg/mol PBSiCB5 (\blacktriangledown , \triangledown). Closed and open symbols in part a indicate two separate experimental runs performed under the same conditions. Arrows indicate the point of cessation of LAOS in selected experiments.

to results in Figure 6 above, upon flow cessation there were modest jumps in orientation, but no discernible trend.

Berghausen and co-workers³⁵ studied shear orientation in nematic side-group LCPs with polymethyl methacrylate (PMMA) backbones and found similar trends in molecular weight as those depicted in our results. Combined rheo-birefringence and rheo-small-angle light scattering (SALS) were used to probe the impact of backbone molecular weight on rheology and structure development. High molecular weight SGLCP samples showed lower birefringence values than low molecular weight samples, indicating lower degrees of orientation were achieved during shear. With increasing molecular weight, it is possible that the shear flow's ability to stretch and orient the backbone is increasingly at odds with its tendency to promote perpendicular alignment of smectic layers. In the isotropic phase, the higher molecular weight PBSiCB5 polymers show increasing signs of an entanglement plateau,²⁴ as found in other SGLCPs,¹⁶ the plateau modulus of this sample is quite small ($G_N^0 = 1.15 \times 10^5$ dyn/cm²),²⁴ corresponding to a large entanglement molecular weight. Chain entanglements, while only likely to be found in high molecular weight samples such as those studied here, could further impede the ability of the smectic layers to orient.

The effect of molecular weight on flow-induced smectic layer alignment was also examined for a higher strain amplitude of 200% (Figure 7b). Comparing parts a and b of Figure 7, it is

clear that the larger strain provides a strong driving force for orientation in each of the molecular weights studied; the highest molecular weight sample (1900K PBSiCB5) now reaches an anisotropy factor near 0.33 after prolonged shearing. These larger strain experiments do, however, reveal interesting differences in behavior upon flow cessation, where anisotropy immediately decreases markedly once the flow is turned off. If the polymer backbone plays a stronger role impeding orientation development in the higher molecular weight samples, it is possible that this rapid decrease reflects a tendency for the orientation to "snap back" due to backbone elasticity once the LAOS promoting the perpendicular alignment is removed.

One puzzle remains when comparing rheological and structural signatures of alignment by LAOS in these materials. Figure 7 clearly demonstrates that lower degrees of smectic layer alignment are realized in the higher molecular weight samples. However, Figure 5 shows that LAOS at 95% strain leads to an appreciable drop in modulus in all samples, even in the highest molecular weight sample where very little layer alignment is achieved at this strain level. While comparison of Figures 4 and 6 suggests a direct connection between layer alignment and modulus reduction, comparison of Figures 5 and 7 suggests that this relationship may be more subtle. One possibility is that LAOS may have sufficient impact on the defect density in the high molecular weight sample to result in substantial modulus reduction even in the absence of significant layer alignment. However, in the absence of direct imaging of the defect structures in these materials, this remains speculative.

4. Conclusions

Combined rheology and in situ X-ray techniques have shown that large amplitude oscillatory shear is an effective means of inducing layer alignment in smectic SGLCPs. X-ray scattering patterns collected during LAOS revealed that shear promotes "perpendicular" smectic layer alignment, where the layer normals accumulate along the vorticity direction. Rheological measurements of the dynamic moduli confirmed that the application of LAOS induces a noticeable decrease in G' , which is in accord with general observations made for layerlike fluids. Larger strains lead to both higher degrees of layer alignment, and sharper reductions in modulus. Increasing the backbone molecular weight makes it harder to achieve high degrees of smectic layer alignment, although it appears that significant alignment may nevertheless be achieved by applying larger strains.

Acknowledgment. We thank Michael. D. Kempe for synthesizing the SGLCPs used in this investigation. We gratefully acknowledge financial support from the Air Force Office of Scientific Research (AFOSR)-LC MURI, the National Science Foundation (Grants DMI-0099542 and DMI-0521823), Fundación Antorchas (Argentina), and CONICET (Argentina). X-ray scattering experiments were conducted at the DuPont-Northwestern-Dow Collaborative Access Team (DND-CAT) Synchrotron Research Center located at Sector 5 of the Advanced Photon Source of Argonne National Laboratory. DND-CAT is supported by the E.I. DuPont de Nemours & Co., the Dow Chemical Company, and the National Science Foundation through Grant DMR-9304725 and the State of Illinois through the Department of Commerce and the Board of Higher Education Grant IBHE HECA NWU 96. Use of the Advanced Photon Source was supported by the U.S. Department of Energy, Basic Energy Sciences, Office of Energy Research, under Contract No. W-31-102-Eng-38.

References and Notes

- (1) Hsu, C. S. *Prog. Polym. Sci.* **1997**, *22*, 829.
- (2) Donald, A. M.; Windle, A. H. *Liquid Crystalline Polymers*; Cambridge University Press: Cambridge, U.K., 1992.
- (3) Larson, R. G. *The Structure and Rheology of Complex Fluids*; Cambridge University Press: New York, 1998.
- (4) Wissbrun, K. F.; Griffin, A. C. *J. Polym. Sci. Pol. Phys.* **1982**, *20*, 1835.
- (5) Zhao, Y.; Roche, P.; Yuan, G. X. *Macromolecules* **1996**, *29*, 4619.
- (6) Gotz, S.; Stille, W.; Strobl, G.; Scheuermann, H. *Ber. Bunsen-Ges. Phys. Chem.* **1993**, *97*, 1315.
- (7) Kannan, R. M.; Kornfield, J. A.; Schwenk, N.; Boeffel, C. *Adv. Mater.* **1994**, *6*, 214.
- (8) Mc Ardle, C. M., Ed. *Side Chain Liquid Crystal Polymers*; Chapman and Hall: New York, 1989.
- (9) Findlay, R. B. *Mol. Cryst. Liq. Cryst.* **1993**, *231*, 137.
- (10) Larson, R. G.; Winey, K. I.; Patel, S. S.; Watanabe, H.; Bruinsma, R. *Rheol. Acta* **1993**, *32*, 245.
- (11) Zentel, R.; Wu, J. S. *Makromol. Chem.* **1986**, *187*, 1727.
- (12) Fabre, P.; Veyssie, M. *Mol. Cryst. Liq. Cryst.* **1987**, *4*, 99.
- (13) Colby, R. H.; Gillmor, J. R.; Galli, G.; Laus, M.; Ober, C. K.; Hall, E. *Liq. Cryst.* **1993**, *13*, 233.
- (14) Kannan, R. M.; Kornfield, J. A.; Schwenk, N.; Boeffel, C. *Macromolecules* **1993**, *26*, 2050.
- (15) Kannan, R. M.; Rubin, S. F.; Kornfield, J. A.; Boeffel, C. *J. Rheol.* **1994**, *38*, 1609.
- (16) Rubin, S. F.; Kannan, R. M.; Kornfield, J. A.; Boeffel, C. *Macromolecules* **1995**, *28*, 3521.
- (17) Wewerka, A.; Viertler, K.; Vlassopoulos, D.; Stelzer, F. *Rheol. Acta* **2001**, *40*, 416.
- (18) Gupta, V. K.; Krishnamoorti, R.; Kornfield, J. A.; Smith, S. D. *Macromolecules* **1996**, *29*, 1359.
- (19) Wiesner, U. *Macromol. Chem. Phys.* **1997**, *198*, 3319.
- (20) Noirez, L.; Lapp, A. *Phys. Rev. Lett.* **1997**, *78*, 70.
- (21) Wiberg, G.; Skytt, M. L.; Gedde, U. W. *Polymer* **1998**, *39*, 2983.
- (22) Hamley, I. W.; Davidson, P.; Gleeson, A. J. *Polymer* **1999**, *40*, 3599.
- (23) Castelletto, V.; Hamley, I. W.; Davidson, P. *Liq. Cryst.* **2004**, *31*, 663.
- (24) Auad, M. L.; Kempe, M. D.; Kornfield, J. A.; Rendon, S.; Burghardt, W. R.; Yoon, K. *Macromolecules* **2005**, *38*, 6946.
- (25) Kannan, R. M.; Kornfield, J. A. *Rheol. Acta* **1992**, *31*, 535.
- (26) Ugaz, V. M.; Burghardt, W. R. *Macromolecules* **1998**, *31*, 8474.
- (27) Burghardt, W. R. *Macromol. Chem. Phys.* **1998**, *199*, 471.
- (28) Hongladarom, K.; Burghardt, W. R. *Macromolecules* **1994**, *27*, 483.
- (29) Cinader, D. K.; Burghardt, W. R. *Macromolecules* **1998**, *31*, 9099.
- (30) Vigild, M. E.; Chu, C.; Sugiyama, M.; Chaffin, K. A.; Bates, F. S. *Macromolecules* **2001**, *34*, 951.
- (31) Alt, D. J.; Hudson, S. D.; Garay, R. O.; Fujishiro, K. *Macromolecules* **1995**, *28*, 1575.
- (32) Zhou, W.-J.; Kornfield, J. A.; Ugaz, V. M.; Burghardt, W. R.; Link, D. R.; Clark, N. A. *Macromolecules* **1999**, *32*, 5581.
- (33) Kirste, R. G.; Ohm, H. G. *Makromol. Chem., Rapid Commun.* **1985**, *6*, 179.
- (34) Noirez, L. *Phys. Rev. Lett.* **2000**, *84*, 2164.
- (35) Berghausen, J.; Fuchs, J.; Richtering, W. *Macromolecules* **1997**, *30*, 7574.
- (36) Caputo, F. E.; Burghardt, W. R. *Macromolecules* **2001**, *34*, 6684.

MA062912C